

Photonic Crystals: A Novel Approach to Enhance the Light Output of Scintillation Based Detectors

Arno Knapitsch^{a,c}, Etienne Auffray^a, C.W. Fabjan^{c,b}, Jean-Louis Leclercq^d, Paul Lecoq^a, Xavier Letartre^d, Christian Seassal^d

^aPH-CMX, CERN, Geneva, Switzerland

^bInstitute of High Energy Physics of the Austrian Academy of Sciences

^cVienna University of Technology

^dUniversit  de Lyon, Institut des Nanotechnologies de Lyon-INL, UMR CNRS 5270 Ecole Centrale de Lyon, F-69134 Ecully, France

Abstract

Future high-energy physics (HEP) experiments as well as next generation medical imaging applications are more and more pushing towards better scintillation characteristics. One of the problems in heavy scintillating materials is related to their high electronic density, resulting in a large index of refraction. As a consequence, most of the scintillation light produced in the bulk material is trapped inside the crystal due to total internal reflection. The same problem also occurs with light emitting diodes (LEDs) and has for a long time been considered as a limiting factor for their overall efficiency. Recent studies have shown that those limits can be overcome by means of light scattering effects of photonic crystals (PhCs). In our simulations we could show light yield improvements between 90 - 110% when applying PhC structures to different scintillator materials. To evaluate the results, a PhC modified scintillator was produced in cooperation with the NIL (Nanotechnology Institute of Lyon). By using silicon nitride (Si_3N_4) as a transfer material for the PhC pattern and a 70 nm thick Indium Tin Oxide (ITO) layer for the electrical conductivity during the lithography process, we could successfully fabricate first samples of PhC areas on top of LYSO crystals.

Key words: Scintillating crystals, photonic crystals, nanolithography, light extraction

1. Introduction

The main limiting factor for the light yield in heavy inorganic scintillators is their high refractive index ($n_{sc} = 1.8 - 2.3$) relative to the ambient medium (typically air or optical grease, $n_{amb} = 1.0 - 1.3$). According to Snell's law, light can only radiate into the ambient medium when the incident angle Θ is smaller than the critical angle $\Theta_c = \arcsin(n_{amb}/n_{crystal})$ (see figure 1). The light extraction efficiency of a plane crystal-air interface can therefore be calculated as shown in the following formula:

$$\eta_{eff} = \frac{1}{2} \int_0^{\Theta_c} \sin\Theta d\Theta \quad (1)$$

In this formula, isotropic light emission is assumed over a solid angle of 4π and Fresnel reflection is neglected. To get the efficiency, light is integrated over all angles which can irradiate into air ($\Theta < \Theta_c$). If we do the calculations for LYSO (cerium-doped Lutetium Yttrium Orthosilicate) which has a refractive index of 1.85, we get an extraction probability of less than 8% at one side of an indefinite plane crystal-air interface (see figure 1). But recent studies have shown that those limits can be overcome due to light scattering effects of photonic crystal (PhC) slabs [1, 2]. In particular, our simulations, which were performed on a full-vectorial Maxwell solver¹ in combination

with a Monte Carlo program for light propagation simulation², were showing an improvement between 90 - 110% in the light yield of different scintillating materials.

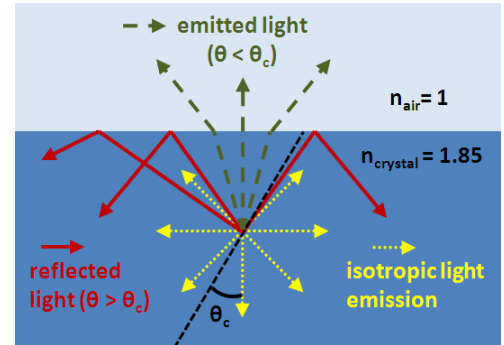


Figure 1: Reflected and emitted light at a crystal-air interface when having isotropic light emission within the crystal. Due to total internal reflection, all light which hits the crystal-air interface with an angle larger than Θ_c can not escape the crystal.

In the second part of this work, an actual sample of a PhC on top of a scintillating crystal (LYSO) was produced. To fabricate the nanometer scale pattern, an electron-beam lithography (EBL) process was used. A silicon nitride (Si_3N_4) layer was applied on top of the scintillator crystal as a pattern transfer material and a scanning electron microscope (SEM) for the

¹CAMFR - (CAvity Modelling FRamework), <http://camfr.sourceforge.net/>

²LITRANI - <http://gentit.home.cern.ch/gentit/litrani/>

patterning of a polymethylmethacrylate (PMMA) resist. By using reactive ion etching for the pattern transfer, we could successfully fabricate several PhC samples with an area of up to $200 \times 200 \mu\text{m}^2$.

2. Simulations

In the simulations, we followed a two step approach. In the first step, we wanted to get an idea about the light yield and the angular light distribution in non-modified scintillators. This was investigated by using a Monte Carlo light ray tracing program. In the second step, the transmission properties of different PhC structures were calculated using a PhC simulation software. A combination of the two programs was then used to optimize the PhC structure towards optimal light extraction properties over all angles of emission and polarization.

2.1. Monte Carlo simulations

Since we were interested in the angular distribution of impinging photons at a crystal-air interface of unstructured material, a Monte Carlo program (LITRANI) was used. LITRANI can simulate optical photons in arbitrary three dimensional geometries of different isotropic or anisotropic materials. When taking the real world measurements of our LYSO crystal sample of $1.3 \times 2.6 \times 8 \text{ mm}^3$ and the absorption, reflection, and diffusion parameters of a Tyvek³ wrapping, the simulations were showing an angular distribution at one of the $1.3 \times 2.6 \text{ mm}^2$ sized sides like shown in figure 2. The light distribution is showing that a large fraction of the light is impinging at an angle larger than Θ_c (see figure 2). Therefore, a PhC which introduces transparency in that region of angles could already bring significant improvement to the overall extraction efficiency. The results were also showing that most of the photons, which are hitting the crystal-air interface at a reflecting angle, are circling within the walls of the crystal and get at some point absorbed by the wrapping or by the crystal itself. We could also see that a small fraction of those photons (5-10%, depending on the crystal wrapping) can escape the crystal at the second or third time they hit the detector coupling side of the crystal.

2.2. Rigorous coupled-wave analysis

In the second part of the simulation, the transmission properties of the PhC slab were computed using a full-vectorial Maxwell solver based on the eigenmode expansion method (CAMFR)⁴. The simulation software, which is available as freeware and runs under Python⁵, uses the rigorous coupled-wave analysis (RCWA) method to calculate the transmission properties of a PhC slab [3]. RCWA is a frequency based method, where the electromagnetic fields are described as a sum over coupled waves. The periodic permittivity function of the PhC structure in RCWA is represented using Fourier harmonics.

³Tyvek is the name of a registered trademark of DuPont; the material consists of flashspun high-density polyethylene fibers.

⁴CAMFR - (CAvity Modeling FRamework), <http://camfr.sourceforge.net/>

⁵<http://www.python.org/>

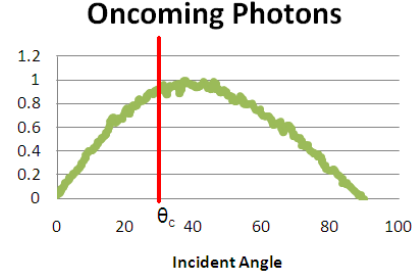


Figure 2: Angular distribution of incident photons at the crystal-air interface for a LYSO crystal of the size $1.3 \times 2.6 \times 8 \text{ mm}^3$. The normalized number of photons is plotted over all possible angles of incidence ($\theta = 0 - 90^\circ$). While almost no light is traveling perpendicular to the surface, the number of photons are increasing with the factor $\sin(\theta)$ up to approximately 40° and then declines again towards 90° .

Each coupled wave in the simulation is then related to a Fourier harmonic, which allows the full vectorial Maxwell's equations to be solved in the frequency domain. The solution is then represented for each harmonic, and therefore has to be summed up over the number of harmonics used in the simulation [4].

This light transmission calculation is then used in combination with the light distribution from the Monte Carlo simulation. In particular, the number of photons we get from the LITRANI simulation is weighted with the transmission of the PhC slab for the given angle. The result can be seen in figure 3, where the light extraction of a plane crystal-air interface and a PhC interface is plotted over all angles of incidence. It can be seen, that we lose some photons in the range of $0 - 30^\circ$ compared to the unstructured crystal, but we gain much more photons in the angular range of $30 - 80^\circ$ due to light diffraction on the PhC grating.

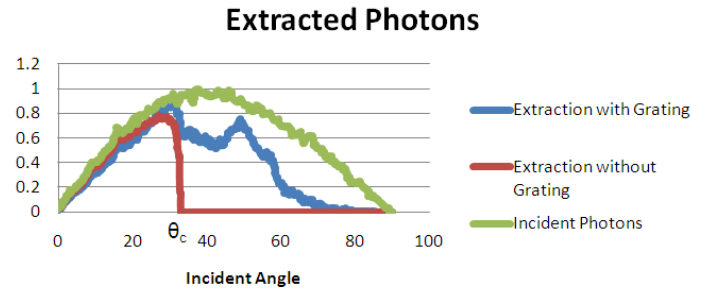


Figure 3: Comparison of extracted photons of a crystal-air interface with- and without PhC grating. The uppermost curve is the angular distribution from figure 2; the curve, that drops to zero for angles higher than Θ_c , indicates the photons from the non-structured crystal surface. From the third curve we can see that, due to the grating of the PhC structure, a large fraction of photons can escape the crystal also at incidence angles larger than Θ_c .

The two simulations were then used to optimize the parameters of the PhC structure (lattice constant, diameter of holes, thickness of the slab). A hexagonal structure of holes showed the best transmission properties compared to lines or squares. The optimized PhC parameters for a LYSO crystal can be seen in figure 4.

3. Lithography

To evaluate the simulation results small PhC areas were created on LYSO scintillators using electron-beam lithography (EBL) and reactive ion etching (RIE). EBL is appropriate for arbitrary 1D or 2D patterns with dimensions corresponding to our designs.

3.1. Sputtering of a transfer material

Since the scintillator material itself can not easily be etched by RIE (reactive ion etching) techniques, a 300 nm layer of Si_3N_4 (silicon nitride) was deposited on top of the crystal as a transfer material for the PhC pattern (see figure 4). The technique used in this case is called sputter deposition. Sputter deposition is one of several methods of physical vapor deposition (PVD). It is widely used in the semiconductor industry to deposit thin films of various materials. In our case ITO (indium tin oxide) is deposited first on our target material (LYSO scintillator) and Si_3N_4 (silicon nitride) on top of the ITO layer (see figure 4). Since ITO is a good electrical conductor and is optically transparent, it is used to get rid of the charges which occur in the electron-beam process. We have chosen to use Si_3N_4 as a pattern transfer material since it has an index of refraction of 1.82 at the emission wavelength of LYSO (420 nm), which is very close to the index of refraction of the LYSO crystal (1.85) and therefore is not disturbing the light extraction by additional diffraction.

3.2. The patterning process

To enable the handling and patterning of the small LYSO samples ($1.3 \times 2.6 \times 8 \text{ mm}^3$) using a standard nanofabrication process, the LYSO samples are embedded in a polydimethylsiloxane matrix (PDMS). The polymethylmethacrylate (PMMA) A4 electro-sensitive resist is then deposited by spin coating. Because of the specific shape and height of the sample, and due to the low thermal conductivity of PDMS, the sample is then baked in an oven at 170 degrees, during 30 minutes. In the patterning process, the electron beam of a Field-Effect Gun SEM (scanning electron microscope) connected to an Elphy Plus external system [5] is used to expose the desired pattern into the resist. The exposed resist is then developed in a mixture of MIBK:IPA(1:1) [6] during 45 seconds.

3.3. Reactive ion etching

The pattern itself is then etched into the substrate by reactive ion etching (RIE). RIE uses a fluorine-containing chemically reactive plasma to transfer the PhC-pattern from the PMMA resist into the Si_3N_4 . The plasma is generated in a vacuum chamber by an electromagnetic field and a mixture of different reactive gases. Since the high-energy ions from the plasma are moving in the direction of the electromagnetic field, an anisotropic etch profile can be created. The anisotropic etching ensures a constant hole diameter from the top to the bottom of the PhC slab, in contrast to the typical isotropic profiles of wet chemical etching.

3.4. Results

The results of the nanolithography can be seen in the SEM-image of figure 5. The lattice constant $a = 340 \text{ nm}$ and the hole diameter $D = 200 \text{ nm}$ of the design could be verified on several small patches of the final sample ($< 200 \times 200 \mu\text{m}^2$). Due to irregularities in the thickness of the mask, the PhC parameters were not equally distributed over larger areas. Depending on the thickness of the resist, the pattern was undergoing over- and underexposure on larger surfaces.

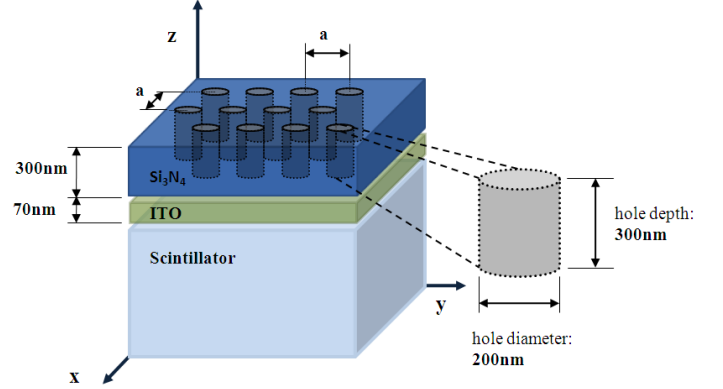


Figure 4: Layout of the PhC structure on top of the scintillator. The holes of the PhC are etched into the Si_3N_4 layer. An about 70 nm thick ITO layer is applied before to ensure good electrical connectivity from the Si_3N_4 to the surrounding area.

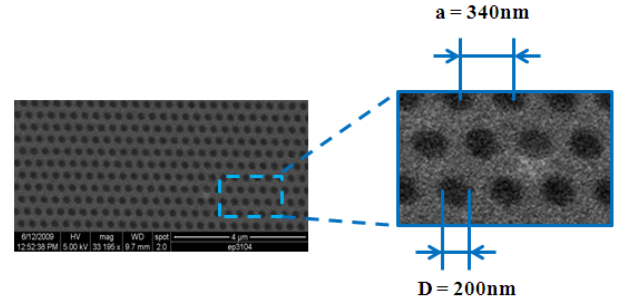


Figure 5: SEM image of a photonic crystal on top of a LYSO scintillator. The PhC pattern consists of hexagonally placed round holes of air embedded in Si_3N_4 . The lattice constant $a = 340 \text{ nm}$ and the hole diameter $D = 200 \text{ nm}$ could be confirmed.

4. Conclusion

From the simulation part of this work a minimum light yield improvement by a factor of about two is expected for different scintillating materials (see table 1). The PhC lattice parameters a and D were optimized for optimal light extraction of the scintillator over all angles of incidence. In the second part of our work several samples of PhC structures could be produced using nanolithography techniques. In the latest sample the parameters of the lithography process could be adapted to produce several small PhC areas on top of a LYSO crystal.

Scintillator material	Relative light-yield improvement	scintillator dimensions	PhC parameters
LYSO	2.08	1.3x2.6x8 mm ³	a=340, D=200
LuAG	1.92	1.3x2.6x8 mm ³	a=430, D=250
BGO	2.11	1.3x2.6x8 mm ³	a=380, D=220
LuYAP	2.10	1.3x2.6x8 mm ³	a=300, D=170

Table 1: Light yield improvement for different scintillators by applying PhC structures at the detector-faced side of the crystal. The PhC lattice parameters are: the lattice constant a , the hole diameter D , and the depth of the holes which was set to 300 nm for all materials (see figure 4).

5. Outlook

Due to irregularities in the deposition of the PMMA resist, we could verify the desired PhC parameters just on small areas ($10 \times 10 \mu\text{m}^2$ to $200 \times 200 \mu\text{m}^2$) in the middle of the scintillator surface. These irregularities could be assigned to border effects due to the small size of the scintillating crystal surface ($1.3 \times 2.6 \text{ mm}^2$). Experiments were showing that the spin coating of the PMMA leads to an accumulation of the resist at the edges of the crystal so that the thickness can get too big for the EBL at these areas. By reducing the overall thickness of the resist layer from the actual 500 nm to 100-150 nm, this effect is believed to vanish. Once this problem is solved, a bigger PhC area is planned for the next sample, which covers a large fraction of the crystal surface (30–50%). The aim for the next sample will therefore be the verification of the simulation results by performing angular distribution and light yield measurements for a PhC covered scintillator.

6. Acknowledgments

Many thanks to Stefano Sgobba and Maud Scheubel from the CERN EN/MME department for their help and support during the SEM observations at the CERN site.

References

- [1] J. Shakya, K.H. Kim, J.Y. Lin, and H.X. Jiang, Enhanced light extraction in III-nitride UV photonic crystal light emitting diodes, *Appl. Phys. Lett.*, 2004, Vol. 85.
- [2] Matthias Kronberger, Etienne Auffray, Paul Lecoq, Optimization of the light extraction from heavy inorganic scintillators. *IEEE Transactions on nuclear science*, vol. 55, No. 3, June 2008.
- [3] M.G. Moharam, T.K. Gaylord, Rigorous coupled-wave analysis of metallic surface-relief gratings, *Journal of the Optical Society*, 1986.
- [4] P. Bienstman, Rigorous and efficient modeling of wavelength scale photonic components, PhD thesis, 2000.
- [5] Raith GmbH, <http://www.raith.com/>
- [6] NANO PMMA and Copolymer Developer, <http://www.microchem.com/products/pdf/pmma.pdf>